

Extending the Higgs sector: an extra singlet

S. I. Godunov^{1,2,a}, A. N. Rozanov³, M. I. Vysotsky^{1,4,5,b}, E. V. Zhemchugov^{1,5,c} 

¹ Institute for Theoretical and Experimental Physics, Moscow 117218, Russia

² Novosibirsk State University, Novosibirsk 630090, Russia

³ The Center for Particle Physics of Marseilles, 13288 Marseille, France

⁴ Moscow Institute of Physics and Technology, Dolgoprudny, Moscow Region 141700, Russia

⁵ Moscow Engineering Physics Institute, Moscow 115409, Russia

Received: 15 September 2015 / Accepted: 27 November 2015

© The Author(s) 2016. This article is published with open access at Springerlink.com

Abstract An extension of the Standard Model with an additional Higgs singlet is analyzed. Bounds on singlet admixture for the 125 GeV h boson from electroweak radiative corrections and data on h production and decays are obtained. The possibility of double h production enhancement at 14 TeV LHC due to a heavy Higgs contribution is considered.

1 Introduction

After the discovery of the Higgs boson [1, 2], all fundamental particles of the Standard Model (SM) have finally been found, and now even passionate adepts of the SM should look for physics beyond it. The pattern of particles we have is rather asymmetric: there are 12 vector bosons, many leptons and quarks with spin 1/2, and only one scalar particle h with mass 125 GeV. Of course, there is only one particle with spin 2 as well, a graviton. However, unlike the spin 2 case, there are no fundamental principles according to which there should exist only one fundamental scalar particle. That is why it is quite probable that there are other still undiscovered fundamental scalar particles in Nature. The purpose of the present paper is to consider the simplest extension of the SM by adding one real scalar field to it. Such an extension of the SM has attracted considerable attention: relevant references can be found in recent papers [3–6]. An extra singlet can provide the first order electroweak phase transition needed for electroweak baryogenesis. It can act as a particle which connects SM particles to Dark Matter. Not going into these (very interesting) applications (see [7–20]), we will study the degree of enhancement of double Higgs production at LHC due to an extra singlet. To do this we should analyze the

bounds on the mass of the additional scalar particle and its mixing with the isodoublet state.

An enhancement of hh production occurs due to the mixing of the SM isodoublet with an additional scalar field which is proportional to the vacuum expectation value (vev) of this field. Thus the isosinglet is singled out: its vev does not violate the custodial symmetry and can be large. For higher representations special care is needed; see Ref. [21] where an introduction of isotriplet(s) in the SM is discussed.

The paper is organized as follows: in Sect. 2 we describe the model and find the physical states. In Sect. 3 we get bounds on the model parameters of the scalar sector from the experimental data on h production and decays and from precision measurements of Z - and W -boson parameters and the t -quark and h masses. In Sect. 4 we discuss double h production at LHC Run 2.

2 The model

Adding to the SM a real field X , we take the scalar fields potential in the following form:

$$V(\Phi, X) = -\frac{m_\Phi^2}{2}\Phi^\dagger\Phi + \frac{m_X^2}{2}X^2 + \frac{\lambda}{2}(\Phi^\dagger\Phi)^2 + \mu\Phi^\dagger\Phi X, \quad (1)$$

where Φ is an isodoublet.¹ Terms proportional to X^3 , X^4 , and $\Phi^\dagger\Phi X^2$ are omitted despite that they are allowed by the demand of renormalizability: we always may assume that they are multiplied by small coupling constants.² Two combinations of the parameters entering (1) are known exper-

^a e-mail: sgodunov@itep.ru

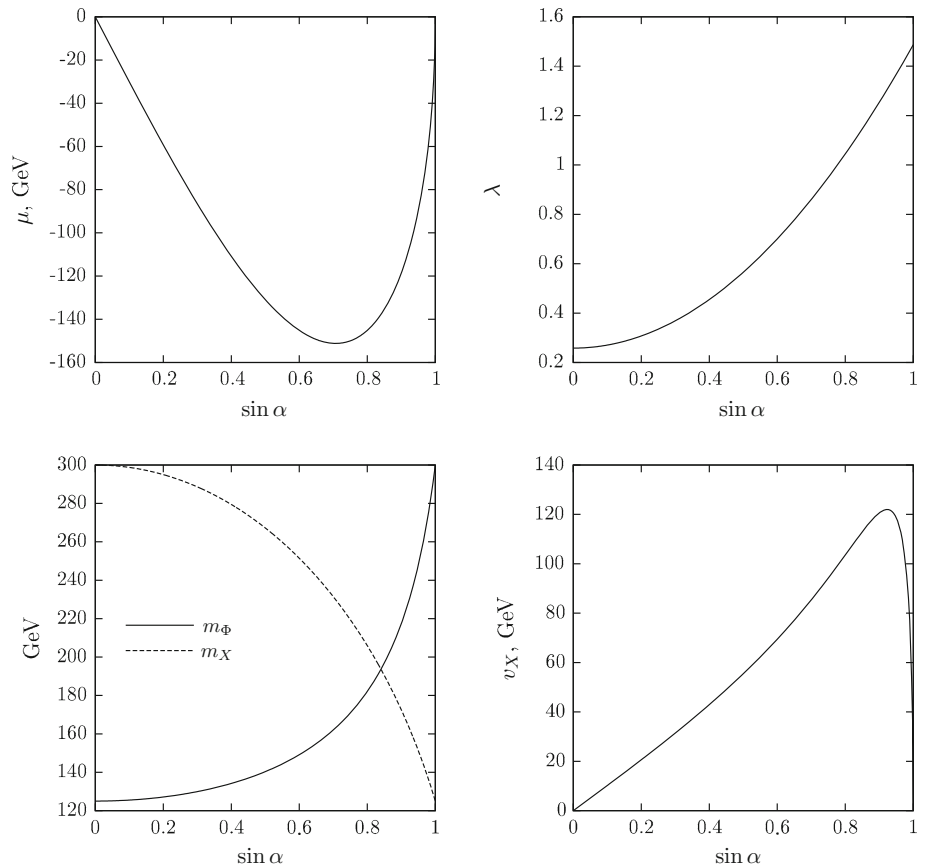
^b e-mail: vysotsky@itep.ru

^c e-mail: zhemchugov@itep.ru

¹ We are grateful to J. M. Frère who brought to our attention that a similar model was considered long ago in [22].

² This choice is justified since the sum of a bare coefficient and radiative correction to it can be chosen to be arbitrary small. Let us note that one

Fig. 1 Dependencies of the model parameters on the mixing angle for $m_H = 300$ GeV



imentally: the mass of one of the two scalar states, h , which equals 125 GeV, and the isodoublet expectation value $v_\phi = 246$ GeV. The two remaining combinations are determined by the mass of the second scalar, H , and the angle, α , which describes the singlet–doublet admixture:

$$\begin{cases} h = \phi \cos \alpha + \chi \sin \alpha, \\ H = -\phi \sin \alpha + \chi \cos \alpha, \end{cases} \quad \begin{cases} \phi = h \cos \alpha - H \sin \alpha, \\ \chi = h \sin \alpha + H \cos \alpha. \end{cases} \quad (2)$$

Since we consider the possibility of double h production enhancement due to the H contribution, $H \rightarrow hh$, we take $m_H > m_h$. Substituting in (1)

$$\Phi = \left(\frac{\phi^+}{\sqrt{2}}(v_\phi + \phi + i\eta) \right), \quad X = v_X + \chi, \quad (3)$$

at the minimum of the potential we get

$$\begin{cases} \lambda v_\phi^2 + 2\mu v_X = m_\phi^2, \\ 2m_X^2 v_X + \mu v_\phi^2 = 0, \end{cases} \quad (4)$$

Footnote 2 continued

always can choose the signs of the coefficients in front of the omitted terms so that the stability of the potential will not be violated. This is possible due to the freedom in the choice of the values of the bare coefficients.

so μ is negative. For the mass matrix using (4) we get

$$M = \begin{pmatrix} V_{\phi\phi} & V_{\phi\chi} \\ V_{\phi\chi} & V_{\chi\chi} \end{pmatrix} = \begin{pmatrix} \lambda v_\phi^2 & \mu v_\phi \\ \mu v_\phi & m_X^2 \end{pmatrix}, \quad (5)$$

where $V_{\phi\chi} \equiv \frac{\partial^2 V}{\partial \phi \partial \chi}, \dots$ The eigenvalues of (5) determine the masses of the scalar particles:

$$m_{h,H}^2 = \frac{1}{2}\lambda v_\phi^2 + \frac{1}{2}m_X^2 \mp \sqrt{\left(\frac{1}{2}\lambda v_\phi^2 - \frac{1}{2}m_X^2\right)^2 + \mu^2 v_\phi^2}, \quad (6)$$

where “−” corresponds to m_h and “+” to m_H . The eigenfunctions are determined by the mixing angle α :

$$\sin 2\alpha = \frac{-2\mu v_\phi}{m_H^2 - m_h^2}, \quad \tan \alpha = \frac{m_h^2 - \lambda v_\phi^2}{\mu v_\phi}. \quad (7)$$

Equation (7) determines μ and λ for the given mixing angle α , while Eq. (6) determines m_X for given α as well. Finally, Eq. (4) determines the values of m_ϕ and v_X . Figure 1 demonstrates the dependencies just described for $m_H = 300$ GeV.

3 Bounds from h production at LHC and electroweak precision observables

ATLAS and CMS Collaborations had detected h production and decays in the reactions

$$pp \rightarrow h \rightarrow f_i, \tag{8}$$

where $f_i, i = 1, 2, \dots, 5$ designate the so-called ‘‘Big five’’ final state channels: $WW^*, ZZ^*, \gamma\gamma, \tau\bar{\tau}, b\bar{b}$. The cross sections of reactions (8) are equal to the Higgs production cross section times the branching ratio of the corresponding decay channel. The quantities μ_i are introduced according to the following definition:

$$\mu_i \equiv \frac{\sigma_{pp \rightarrow h} \cdot \Gamma_{h \rightarrow f_i} / \Gamma_h}{(\sigma_{pp \rightarrow h} \cdot \Gamma_{h \rightarrow f_i} / \Gamma_h)_{SM}}. \tag{9}$$

According to the ATLAS and CMS results, all μ_i are compatible with one within experimental and theoretical accuracy. It means that no New Physics are up to now observed in h production and decays.

In the model with an extra isosinglet, production and decay probabilities of h equal that in the SM multiplied by a factor $\cos^2 \alpha$, which is why we have

$$\mu_i = \cos^2 \alpha, \tag{10}$$

and existing bounds on μ_i are translated into bounds on the mixing angle α . Taking into account all measured production and decay channels, for the average values experimentalists obtain [23,24]

$$\text{ATLAS: } \mu = 1.30^{+0.18}_{-0.17}, \tag{11}$$

$$\begin{aligned} \text{CMS: } \mu &= 1.00^{+0.14}_{-0.13} \\ &= \pm 0.09(\text{stat.})^{+0.08}_{-0.07}(\text{theor.}) \pm 0.07(\text{syst.}). \end{aligned} \tag{12}$$

Let us stress that the theoretical uncertainty in the calculation of $pp \rightarrow h$ production cross section at LHC does not allow one to reduce substantially the uncertainty in the value of μ . The bounds from electroweak precision observables (EWPO) are not affected by this particular uncertainty.

We fit experimental data with the help of LEPTOP program [25–29] using $m_h = 125.14$ GeV. The result of the SM fit which accounts for the h mass measurement is shown in Table 1. The quality of the fit is characterized by the χ^2 value

$$\chi^2/n_{\text{d.o.f.}} = 19.6/13. \tag{13}$$

Higgs boson contributions to electroweak observables at one loop are described in LEPTOP by the functions $H_i(h) = H_i(m_h^2/m_Z^2)$. In the case of an extra singlet the following substitution should be performed:

$$H_i(h) \rightarrow \cos^2 \alpha H_i(h) + \sin^2 \alpha H_i(H), \quad H = m_H^2/m_Z^2. \tag{14}$$

The same substitution should be made for the functions $\delta_4 V_i(t, h), t = m_t^2/m_Z^2$, which describe two loops radiative corrections enhanced as m_t^4 .

In two loops a quadratic dependence on the Higgs mass appears which is described by the functions $\delta_5 V_i$. The calculation of these corrections in the case of an extra singlet Higgs

Table 1 EWPO fit of the Standard Model

Observable	Experimental value	Standard Model	Pull
Γ_Z (GeV)	2.4952 (23)	2.4966 (14)	−0.5895
σ_h (nb)	41.541 (37)	41.475 (14)	1.7746
R_l	20.771 (25)	20.744 (18)	1.0831
A_{FB}^l	0.0171 (10)	0.0165 (2)	0.6572
A_τ	0.1439 (43)	0.1484 (7)	−1.0452
R_b	0.2163 (7)	0.2158 (0)	0.7699
R_c	0.1721 (30)	0.1722 (0)	−0.0277
A_{FB}^b	0.0992 (16)	0.1040 (5)	−3.0303
A_{FB}^c	0.0707 (35)	0.0744 (4)	−1.0565
$s_l^2 (Q_{\text{FB}})$	0.2324 (12)	0.2313 (1)	0.8771
A_{LR}	0.1514 (22)	0.1484 (7)	1.3822
A_b	0.923 (20)	0.9349 (1)	−0.5941
A_c	0.670 (27)	0.6685 (3)	0.0567
M_W (GeV)	80.3846 (146)	80.3725 (67)	0.8322
m_t (GeV)	173.24 (95)	174.32 (89)	−1.1370
$1/\bar{\alpha}$	128.954 (48)	129.023 (37)	−1.4378

is not easy. However, even for a 1000 GeV Higgs these corrections are small. We checked that corrections to the values of $\sin \alpha$ due to $\delta_5 V_i$ terms in Fig. 2 are less than 10^{-3} .

The bounds from EWPO on the singlet model parameters are presented in Fig. 2a. A χ^2 minimum is reached at $\sin \alpha = 0$, $m_H = 150$ GeV, which is the minimum value allowed for m_H in the fit. Experimental data are avoiding a heavy Higgs. The value of χ^2 at the minimum coincides with the SM result (13). Lines of constant χ^2 correspond to $\Delta\chi^2 = 1, 4, 9, \dots$. The probabilities that $(\sin \alpha, m_H)$ values are below these lines are 39, 86, 98.9 %, ...³

Bounds accounting for both EWPO and direct h production data (11), (12), are shown in Fig. 2b. We see that for a heavy H the bounds from EWPO dominate, while for a light H the measurement of μ is more important.

4 h, H , and hh production at LHC

The main purpose of this section is to find what enhancement of double Higgs production cross section is possible with enlarged Higgs sector. Let us recall that in the SM the double h production cross section is very small. According to the recent result [30], at $\sqrt{s} = 14$ TeV $\sigma^{\text{NNLO}}(pp \rightarrow hh) = 40$ fb with a $10 \div 15$ % accuracy. We will demonstrate that an enlarged Higgs sector allows one to strongly enhance double h production.

The cross section of H production at LHC equals that for the SM Higgs production (for $(m_h)_{\text{SM}} = m_H$) multiplied by $\sin^2 \alpha$. We take the cross section of the SM Higgs production at NNLO from Table 3 of [31]. In order to obtain the cross section of resonant hh production in H decays we should multiply the cross section of H production by $\text{Br}(H \rightarrow hh)$.

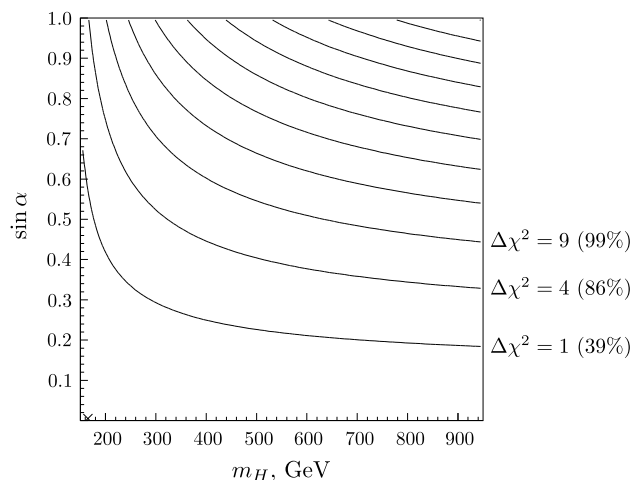
Let us consider H decays. Decays to hh, W^+W^-, ZZ , and $t\bar{t}$ dominate. For the Hhh coupling we obtain

$$\begin{aligned} \Delta\mathcal{L}_{Hhh} &= \left[\frac{3}{2} \lambda v_\phi \cos^2 \alpha \sin \alpha - \frac{\mu}{2} \cos \alpha (1 - 3 \sin^2 \alpha) \right] Hh^2 \\ &= \frac{2m_h^2 + m_H^2}{2v_\phi} \sin \alpha \cos^2 \alpha Hh^2 \\ &\equiv g_{Hhh} Hh^2, \end{aligned} \tag{15}$$

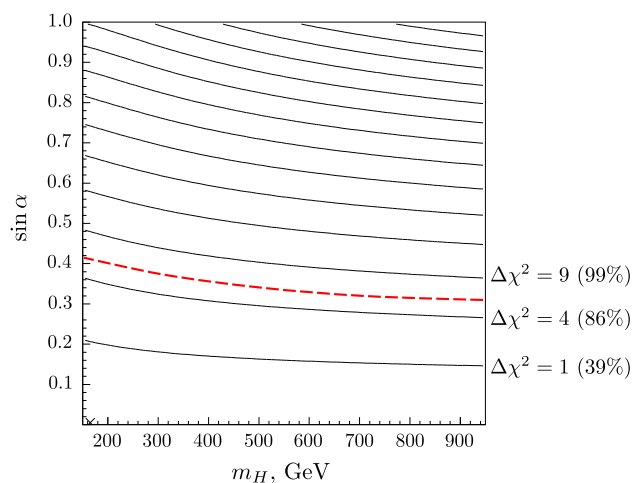
thus

$$\Gamma_{H \rightarrow hh} = \frac{g_{Hhh}^2}{8\pi m_H} \sqrt{1 - \left(\frac{2m_h}{m_H}\right)^2}. \tag{16}$$

³ Let us note that if a subset of the experimental data from Table 1 is fitted, then the allowed domains of the $(\sin \alpha, m_H)$ values will be larger than those presented in Fig. 2a. Here we disagree with the statement made in [4] that the fit of only one observable (m_W) allows one to set the strongest constraint on $(\sin \alpha, m_H)$.



(a) Bounds from electroweak precision observables.



(b) Bounds from both electroweak precision observables and signal strength measurements (11), (12). The dashed line corresponds to $\Delta\chi^2 = 5.99$; the probability that numerical values of $(m_H, \sin \alpha)$ are below it equals 95% (compare with Ref. [6], eq. (23)).

Fig. 2 Bounds on the singlet model parameters

Decays to $W^+W^-, ZZ, t\bar{t}$ occur through isodoublet admixture in H :

$$\begin{aligned} \Delta\mathcal{L} &= \frac{2m_W^2}{v_\phi} \sin \alpha HW^+W^- + \frac{m_Z^2}{v_\phi} \sin \alpha HZ^2 \\ &\quad + \frac{m_t}{v_\phi} \sin \alpha Ht\bar{t} \\ &\equiv g_{HW} HW^+W^- + \frac{1}{2} g_{HZ} HZ^2 + g_{Ht} Ht\bar{t}, \end{aligned} \tag{17}$$

thus

$$\begin{aligned} \Gamma_{H \rightarrow W^+W^-} &= \frac{g_{HW}^2 m_H^3}{64\pi m_W^4} \left[1 - 4 \frac{m_W^2}{m_H^2} + 12 \frac{m_W^4}{m_H^4} \right] \\ &\quad \times \sqrt{1 - \left(\frac{2m_W}{m_H}\right)^2}, \end{aligned} \tag{18}$$

Fig. 3 Decay widths and branching ratios of the heavy Higgs boson for $m_H = 300$ GeV

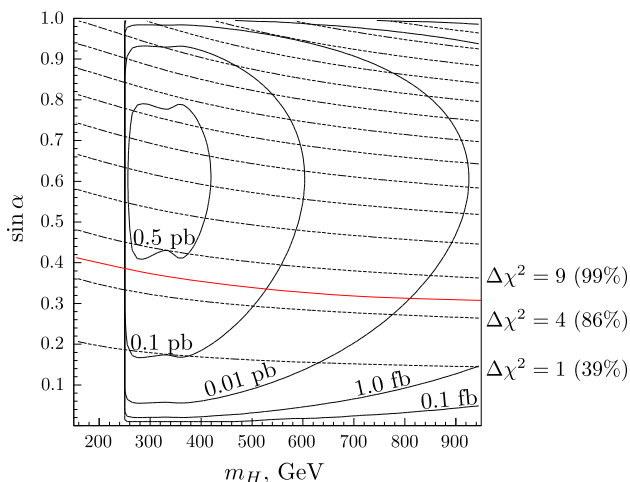
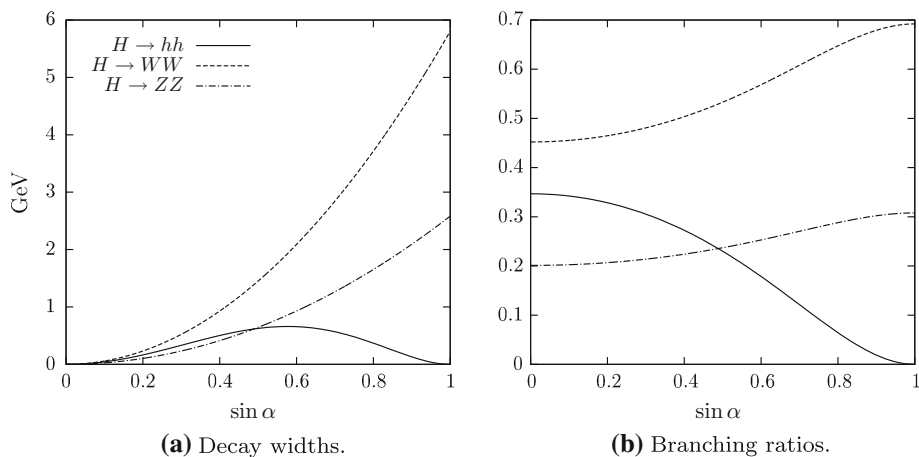


Fig. 4 Contour plot of $\sigma(pp \rightarrow H \rightarrow hh)$ for $\sqrt{s} = 14$ TeV. In this figure we neglect small effects of $H \rightarrow hh^*$

$$\Gamma_{H \rightarrow ZZ} = \frac{g_{HZZ}^2 m_H^3}{128\pi m_Z^4} \left[1 - 4 \frac{m_Z^2}{m_H^2} + 12 \frac{m_Z^4}{m_H^4} \right] \quad (19)$$

$$\times \sqrt{1 - \left(\frac{2m_Z}{m_H} \right)^2},$$

$$\Gamma_{H \rightarrow t\bar{t}} = \frac{3g_{Ht\bar{t}}^2 m_H}{8\pi} \left[1 - \left(\frac{2m_t}{m_H} \right)^2 \right]^{\frac{3}{2}}. \quad (20)$$

The dependences of the widths and branching ratios of H decays on the mixing angle α for $m_H = 300$ GeV are shown in Fig. 3.

For the cross section of the reaction $pp \rightarrow H \rightarrow hh$ we have

$$\sigma(pp \rightarrow H \rightarrow hh) = \sigma(pp \rightarrow h)_{SM} \cdot \sin^2 \alpha \cdot \text{Br}(H \rightarrow hh), \quad (21)$$

the lines of constant cross section are shown in Fig. 4 (compare Fig. 4 in [6]). $H \rightarrow ZZ$ decay can be used in order to find H ; its cross section divided by that for the SM Higgs boson with $(m_h)_{SM} = m_H$ is

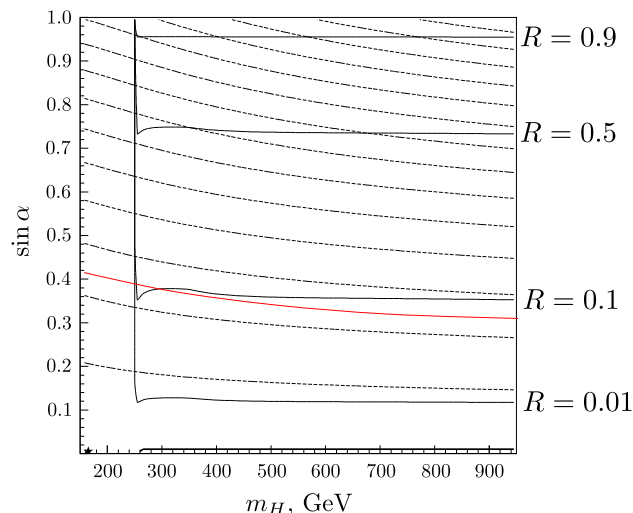


Fig. 5 Contour plot of $R \equiv \frac{\sigma(pp \rightarrow H) \text{Br}(H \rightarrow ZZ)}{(\sigma(pp \rightarrow h) \text{Br}(h \rightarrow ZZ))_{SM}}$. In the calculation of R we assume $m_H > 2m_h$

$$R \equiv \frac{\sigma(pp \rightarrow H) \cdot \text{Br}(H \rightarrow ZZ)}{(\sigma(pp \rightarrow h) \cdot \text{Br}(h \rightarrow ZZ))_{SM}}$$

$$= \frac{\sin^4 \alpha}{\sin^2 \alpha + \frac{\Gamma(H \rightarrow hh)}{\Gamma_{SM}}}. \quad (22)$$

Contour plot of R is presented in Fig. 5. Let us note that R does not depend on \sqrt{s} . See also $\sigma(pp \rightarrow H) \cdot \text{Br}(H \rightarrow ZZ)$ for different values of $\sin \alpha$ in Fig. 6.

5 Conclusions

In the models with extended Higgs sector strong resonant enhancement of double Higgs production is possible, which makes the search of the $pp \rightarrow hh$ reaction at Run 2 LHC especially interesting. According to Fig. 4 the cross section of the $pp \rightarrow H \rightarrow hh$ reaction can be as large as 0.5 pb, ten times larger than the SM value.

The search for a H boson can go in the same way as for the heavy SM boson h . The probability of H observation is

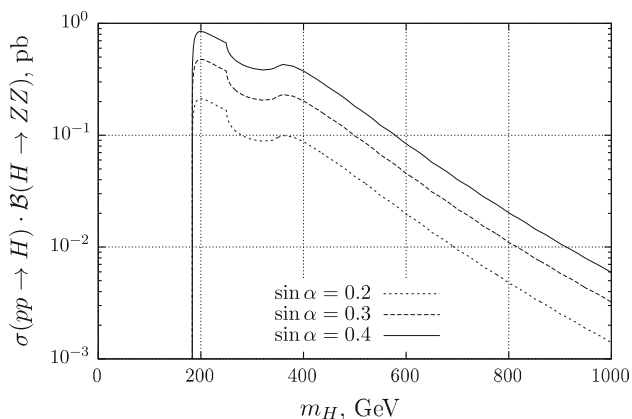


Fig. 6 $\sigma(pp \rightarrow H) \cdot \text{Br}(H \rightarrow ZZ)$ for different values of the mixing angle for $\sqrt{s} = 14$ TeV

diminished compared to that of h because of (a) suppression of H production cross section by the factor $\sin^2 \alpha \leq 0.2$; and (b) suppression of $\text{Br}(H \rightarrow ZZ)$ because of an additional $H \rightarrow hh$ decay mode. Taking these two factors into account, we get a suppression of about a factor 10 of the $pp \rightarrow H \rightarrow ZZ$ process probability compared to that for the SM Higgs boson (see Fig. 5).

Results for the search of the Higgs-like boson in ZZ decay mode by CMS can be found in [32], Figure 18, [33], Figure 7, and by ATLAS in [34], Figure 12. Comparing it with our Fig. 5, we observe that the experimental data start to be sensitive to the singlet model expectation for maximally allowed values of the mixing angle α .

Acknowledgments S. G., M. V. and E. Zh. are partially supported under the grants RFBR No. 14-02-00995 and NSH-3830.2014.2. S. G. and E. Zh. are also supported by MK-4234.2015.2. In addition, S. G. is supported by RFBR under grant 16-32-60115, Dynasty Foundation and by the Russian Federation Government under Grant No. 11.G34.31.0047.

Open Access This article is distributed under the terms of the Creative Commons Attribution 4.0 International License (<http://creativecommons.org/licenses/by/4.0/>), which permits unrestricted use, distribution, and reproduction in any medium, provided you give appropriate credit to the original author(s) and the source, provide a link to the Creative Commons license, and indicate if changes were made. Funded by SCOAP³.

References

1. The ATLAS Collaboration, Phys. Lett. B **716**, 1 (2012)
2. The CMS Collaboration, Phys. Lett. B **716**, 30 (2012)
3. C.-Y. Chen, S. Dawson, I.M. Lewis, Phys. Rev. D **91**, 035015 (2015). [arXiv:1410.5488](https://arxiv.org/abs/1410.5488)
4. T. Robens, T. Stefaniak, Eur. Phys. J. C **75**, 104 (2015). [arXiv:1501.02234](https://arxiv.org/abs/1501.02234)
5. V. Martin-Lozano, J.M. Moreno, C.B. Park, JHEP **1508**, 004 (2015). [arXiv:1501.03799](https://arxiv.org/abs/1501.03799)
6. A. Falkowski, C. Gross, O. Lebedev, JHEP **1505**, 057 (2015). [arXiv:1502.01361](https://arxiv.org/abs/1502.01361)
7. S. Profumo, M.J. Ramsey-Musolf, G. Shaughnessy, JHEP **0708**, 010 (2007). [arXiv:0705.2425](https://arxiv.org/abs/0705.2425)
8. V. Barger, P. Langacker, M. McCaskey, M.J. Ramsey-Musolf, G. Shaughnessy, Phys. Rev. D **77**, 035005 (2008). [arXiv:0706.4311](https://arxiv.org/abs/0706.4311)
9. V. Barger, P. Langacker, M. McCaskey, M.J. Ramsey-Musolf, G. Shaughnessy, Phys. Rev. D **79**, 015018 (2009). [arXiv:0811.0393](https://arxiv.org/abs/0811.0393)
10. M. Gonderinger, Y. Li, H. Patel, M.J. Ramsey-Musolf, JHEP **1001**, 053 (2010). [arXiv:0910.3167](https://arxiv.org/abs/0910.3167)
11. M. Kadastik, K. Kannike, A. Racioppi, M. Raidal, JHEP **1205**, 061 (2012). [arXiv:1112.3647](https://arxiv.org/abs/1112.3647)
12. M. Gonderinger, H. Lim, M.J. Ramsey-Musolf, Phys. Rev. D **86**, 043511 (2012). [arXiv:1202.1316](https://arxiv.org/abs/1202.1316)
13. C. Caillol, B. Clerbaux, J.M. Frère, S. Mollet, Eur. Phys. J. Plus **129**, 93 (2014). [arXiv:1304.0386](https://arxiv.org/abs/1304.0386)
14. E. Gabrielli, M. Heikinheimo, K. Kannike et al., Phys. Rev. D **89**, 1, 015017 (2014). [arXiv:1309.6632](https://arxiv.org/abs/1309.6632)
15. L. Basso, O. Fischer, J.J. van der Bij, Phys. Lett. B **730**, 326–331 (2014). [arXiv:1309.8096](https://arxiv.org/abs/1309.8096)
16. J.M. No, M.J. Ramsey-Musolf, Phys. Rev. D **89**, 9, 095031 (2014). [arXiv:1310.6035](https://arxiv.org/abs/1310.6035)
17. J. de Blas, M. Chala, M. Pérez-Victoria, J. Santiago, JHEP **1504** 078, CERN-PH-TH-2014-264 (2015). [arXiv:1412.8480](https://arxiv.org/abs/1412.8480)
18. S. Profumo, M.J. Ramsey-Musolf, C.L. Wainwright, P. Winslow, Phys. Rev. D **91**, 3, 035018 (2015). [arXiv:1407.5342](https://arxiv.org/abs/1407.5342)
19. M. Gorbahn, J.M. No, V. Sanz, JHEP **1510**, 036 (2015). [arXiv:1502.07352](https://arxiv.org/abs/1502.07352)
20. D. Curtin, P. Meade, Ch.-T. Yu, JHEP **1411**, 127 (2014). [arXiv:1409.0005](https://arxiv.org/abs/1409.0005)
21. S. Godunov, M. Vysotsky, E. Zhemchugov, J. Exp. Theor. Phys. **120**(3), 369–375 (2015). [arXiv:1408.0184](https://arxiv.org/abs/1408.0184)
22. A. Hill, J.J. van der Bij, Phys. Rev. D **36**, 3463 (1987)
23. The ATLAS Collaboration, in *Proc. of the 49th Rencontres de Moriond on Electroweak Interactions and Unified Theories*, La Thuile, Italy, 15–22 March 2014. ATLAS-CONF-2014-009 (2014)
24. The CMS Collaboration, Eur. Phys. J. C **75**, 5, 212 (2015). [arXiv:1412.8662](https://arxiv.org/abs/1412.8662). (CERN-PH-EP-2014-288, CMS-HIG-14-009)
25. V.A. Novikov, L.B. Okun, A.N. Rozanov, M.I. Vysotsky, Rep. Progr. Phys. **62**, 1275 (1999)
26. V.A. Novikov, L.B. Okun, A.N. Rozanov, M.I. Vysotsky, Phys. Usp. **39**, 503 (1996)
27. V.A. Novikov, L.B. Okun, A.N. Rozanov, M.I. Vysotsky, Usp. Fiz. Nauk **166**, 539 (1996)
28. Electroweak Working Group Report Dmitri Yu. Bardin et al. Sep (1997). 158 pp. CERN-95-03A, CERN-YELLOW-95-03A
29. V.A. Novikov, L.B. Okun, A.N. Rozanov, M.I. Vysotsky, CPPM-95-1, ITEP 19/95. [arXiv:hep-ph/9503308](https://arxiv.org/abs/hep-ph/9503308)
30. D. de Florian, J. Mazzitelli, PoS **LL2014**, 029 (2014). [arXiv:1405.4704](https://arxiv.org/abs/1405.4704). (DESY 14-080 / LPN 14-073)
31. S. Dittmaier, C. Mariotti, G. Passarino et al., *Handbook of LHC Higgs Cross Sections: 1. Inclusive Observables*. (CERN, Geneva 2011), CERN-2011-002. [arXiv:1101.0593](https://arxiv.org/abs/1101.0593)
32. The CMS Collaboration, Phys. Rev. D **89**, 092007. CMS-HIG-13-002. CERN-PH-EP-2013-220 (2014). [arXiv:1312.5353](https://arxiv.org/abs/1312.5353)
33. The CMS Collaboration, JHEP **1510**, 144. CMS-HIG-13-031. CERN-PH-EP-2015-074 (2015). [arXiv:1504.00936](https://arxiv.org/abs/1504.00936)
34. The ATLAS Collaboration, CERN-PH-EP-2015-154 (2015). [arXiv:1507.05930](https://arxiv.org/abs/1507.05930). (see also CERN-PH-EP-2015-185, [arXiv:1509.0038](https://arxiv.org/abs/1509.0038))